The structure of the solution obtained with Reynolds-stress-transport models at the free-stream edges of turbulent flows

J.-B. Cazalbou[a] and P. Chassaing[b]
ENSICA, 1 place Émile Blouin, 31056 Toulouse cedex 5, France

(Received 29 June 2001; accepted 9 October 2001)

The behavior of Reynolds-stress-transport models at the free-stream edges of turbulent flows is investigated. Current turbulent-diffusion models are found to produce propagative (possibly weak) solutions of the same type as those reported earlier by Cazalbou, Spalart, and Bradshaw [Phys. Fluids **6**, 1797 (1994)] for two-equation models. As in the latter study, an analysis is presented that provides qualitative information on the flow structure predicted near the edge if a condition on the values of the diffusion constants is satisfied. In this case, the solution appears to be fairly insensitive to the residual free-stream turbulence levels needed with conventional numerical methods. The main specific result is that, depending on the diffusion model, the propagative solution can force turbulence toward definite and rather extreme anisotropy states at the edge (one- or two-component limit). This is not the case with the model of Daly and Harlow [Phys. Fluids **13**, 2634 (1970)]; it may be one of the reasons why this ''old'' scheme is still the most widely used, even in recent Reynolds-stress-transport models. In addition, the analysis helps us to interpret some difficulties encountered in computing even very simple flows with Lumley's pressure-diffusion model [Adv. Appl. Mech. **18**, 123 (1978)]. A new realizability condition, according to which the diffusion model should not globally become ''anti-diffusive,'' is introduced, and a recalibration of Lumley's model satisfying this condition is performed using information drawn from the analysis. © *2002 American Institute of Physics.* [DOI: 10.1063/1.1423933]

I. INTRODUCTION

The singular behavior of popular turbulence models at the edge of turbulent regions has often been reported.[1–4] It is related to the vanishing of the *variable* diffusivity used in gradient-transport modeling of turbulent diffusion. It has been shown by Spalart and Allmaras[5] for their one-equation model, and by Cazalbou, Spalart, and Bradshaw[6] for most two-equation models, that the singularity (discontinuity to some order of the transported variables) is the result of the propagative character of the solution. Such solutions occur when turbulent diffusion is the dominant term in the budget of the modeled equations in this region. This is so for all the models considered in Refs. 5 and 6, provided that some special inequalities between the model constants are satisfied. The discontinuity corresponds to a turbulent front located at a finite distance from the turbulence-generating region, and the front proceeds in the undisturbed fluid with a finite ''propagation'' velocity. It is interesting to note that this peculiar mathematical behavior of the gradient-transport model is revealed in a situation which is rather far from the framework in which the model is introduced (a fully turbulent fluid and some crude analogy between the macroscopic-momentum transport by molecular motion and the mean-momentum transport by turbulent velocity fluctuations) but possesses amazing similarities to what is observed in real flow. As a matter of fact, the interface between turbulent (vortical) fluid and nonturbulent fluid in unconfined space at high Reynolds number is by no means gradual. Instantaneously, it is sharp: the width of the transition ''superlayer'' is proportional to molecular viscosity which is small; and highly contorted:[7] the size of the turbulent bulges scales on that of the large turbulent eddies. It is, therefore, barely conceivable that even rare turbulent bulges could reach infinity (or at least a distance significantly larger than a characteristic length scale of the mean flow), and consequently, statistics of the *vortical* fluctuations should reach *strictly* their free-stream values at a finite distance from the turbulence-generating region. Another positive consequence of the propagative character of the solution is of computational nature: With most models and a conventional numerical setup, one cannot use strictly zero values for the turbulent quantities in the free-stream, but the propagative solution ensures that the result in the core of the turbulent layer is virtually independent of these values provided that they are reasonably small (see Ref. 6).

To our knowledge, the existence of propagative solutions at the second-order-closure level has not been demonstrated although careful computations of simple shear layers seem to support this idea. In this paper, we generalize the analysis of Cazalbou *et al.*[6] to the case of Reynolds-stress-transport models. One will see that such solutions do exist for the most popular diffusion models, and strongly constrain the structure (in terms of anisotropy) of the predicted turbulence at free-stream edges.

Considering the characteristics of anisotropy in this re-

[a]Author to whom correspondence should be addressed. Telephone: (33) 5 61 61 86 59; Fax: (33) 5 61 61 86 63. Electronic mail: cazalbou@ensica.fr
[b]Also at: INPT-ENSEEIHT-Institut de Mécanique des Fluides de Toulouse UMR 5502 CNRS.

TABLE I. Evaluation of $\overline{w_T^2}/k_T$ for turbulent fluctuations in the turbulence-generating region and at the mean interface for various simple-shear flows; the arrow ($\nearrow$, $\rightarrow$, $\searrow$) indicates the trend at the mean interface (either increasing, roughly constant or decreasing).

	Source region	Mean interface
Plane wake (Ref. 9)	0.54 (half-velocity defect width)	0.61 ($\nearrow$)
Plane jet (Ref. 10)	0.38 (half-velocity width)	0.31 ($\searrow$)
Plane mixing layer (Ref. 11)	0.46 (centerline)	High-speed side: 0.67 ($\nearrow$) Low-speed side: 0.43 ($\rightarrow$)
Wall boundary layer (Ref. 12)	0.41 ($y=0.37\delta$)	0.6–0.66 ($\nearrow$)
Wall boundary layer (Ref. 13)	0.36–0.4 ($y=0.1\delta$)	0.43–0.5 ($\nearrow$)

gion, a meaningful comparison between the results of the forthcoming analysis and experiment is not straightforward. The problem stems from the fact that the flow is highly intermittent there, and consequently, conventional statistics contain contributions from both the actual turbulent fluctuations on one side of the instantaneous interface and irrotational fluctuations on the other side. The characteristics of these two kinds of fluctuations are essentially distinct: The irrotational fluctuations are barely dissipative; according to Phillips,[8] they do not produce shear stress, and display an anisotropy that favors the component normal to the mean interface (the corresponding ''Reynolds stress'' amounts to the sum of the other two). As the free stream is approached, their contribution to the conventional statistics increases so that the latter tend to reflect the characteristics of the irrotational fluctuations. Therefore, it seems reasonable to consider that predictions should be compared with measurements of the turbulent *dissipative* and *shear-producing* fluctuations. Information on these fluctuations can be obtained from experiment when conditional averaging is used. Data inferred from such experiments[9–13] are presented in Table I. The statistics we used involve only the actual *turbulent* fluctuations: $\overline{w_T^2}$ is the corresponding normal Reynolds stress along z, the direction of propagation, and k_T is the corresponding turbulent kinetic energy. For each configuration, the ratio $\overline{w_T^2}/k_T$ has been evaluated in the turbulence-generating region and at the mean interface. According to these data, there is no evidence that a definite anisotropy state should be reached in the region of the mean interface. Instead, the value of $\overline{w_T^2}/k_T$ there seems to be closely connected with its value in the ''source'' region, and also—with the exceptions of the plane jet and the low-speed side of the mixing layer—seems to tend toward the value corresponding to isotropy (2/3) or, further, to the equilibrium state observed in steady diffusive turbulence (0.75–0.84, see De Silva and Fernando[14] for instance). Note that the two exceptions cited above correspond to measurements in a region where the mean velocity goes to zero and that reliable hot-wire data are usually difficult to obtain in such conditions.

The analysis presented in this paper is divided into two parts. In a first step (Sec. II), the model problem is studied in the absence of mean shear with the case of turbulence propagating from a steady plane source. In a second step (Sec. III) the scope of the analysis is extended to simple-shear flows with the case of a time-evolving mixing layer. In both cases, the behavior of several turbulent-diffusion models is examined, and numerical calculations are presented to support the conclusions of the analysis. In some circumstances, it has not been possible to obtain numerical solutions with Lumley's pressure-diffusion model, Sec. IV introduces a new realizability condition, which is violated by this scheme with the original values of the model constants. A recalibration of the model based on intermediate results of the analysis is then presented.

From now on, we shall use conventional statistics (the averages will be denoted by overbars) assuming that conventional turbulence modeling neglects the irrotational fluctuations and also their interactions with the mean flow and the actual turbulent fluctuations.

II. SHEAR-FREE PROPAGATING TURBULENCE

When a source of turbulence is activated in still fluid, turbulent transport causes progressive contamination of the fluid behind a turbulent–nonturbulent interface. This situation allows the characteristics of the flow in the vicinity of the interface to be examined in the absence of mean-velocity gradient. Here, we consider an incompressible fluid filling the whole space. At some initial time, high-Reynolds-number turbulence is generated in the plane $z=0$, and then remains statistically steady and homogeneous in this plane. This flow configuration will be referred to as that of *turbulence propagating from a steady plane source*. At any time in the contaminated region, the statistics are homogeneous in the planes perpendicular to z, and the exact transport equation for the Reynolds stress $\overline{u_i u_j}$ (u_i denotes the velocity fluctuation along x_i) can be written in the simplified form

$$\frac{\partial \overline{u_i u_j}}{\partial t} = \underbrace{\frac{\partial}{\partial z}\left(-\overline{u_i u_j w}\right)}_{D_{ij}^u} + \underbrace{\frac{\partial}{\partial z}\left(-\frac{\overline{p u_i}}{\rho}\delta_{j3} - \frac{\overline{p u_j}}{\rho}\delta_{i3}\right)}_{D_{ij}^p} + \underbrace{\overline{\frac{p}{\rho}\left(\frac{\partial u_j}{\partial x_i} + \frac{\partial u_i}{\partial x_j}\right)}}_{\Pi_{ij}} - \underbrace{2\nu\overline{\left(\frac{\partial u_i}{\partial x_k}\frac{\partial u_j}{\partial x_k}\right)}}_{\epsilon_{ij}},$$

where D_{ij}^u and D_{ij}^p are the turbulent-diffusion terms by velocity and pressure fluctuations respectively, Π_{ij} is the pressure-strain correlation, and ϵ_{ij} the dissipation term with $\epsilon=\epsilon_{ii}/2$. Viscous diffusion is neglected owing to the hypothesis of high turbulence Reynolds number. Turbulence pro-

TABLE II. Definition of the Reynolds-stress diffusion schemes used.

Daly–Harlow (Ref. 15)	$-\overline{u_i u_j u_k}=C_s\frac{k}{\epsilon}\overline{u_k u_l}\,\frac{\partial\overline{u_i u_j}}{\partial x_l}$
Hanjalić–Launder (Ref. 16)	$-\overline{u_i u_j u_k}=C_s\frac{k}{\epsilon}G_{ijk}$
Mellor–Herring (Ref. 17)	$-\overline{u_i u_j u_k}=C_s\frac{k^2}{\epsilon}\left(\frac{\partial\overline{u_i u_j}}{\partial x_k}+\frac{\partial\overline{u_i u_k}}{\partial x_j}+\frac{\partial\overline{u_j u_k}}{\partial x_i}\right)$
Lumley (Ref. 18) (D^u_{ij})	$-\overline{u_i u_j u_k}=C_{s1}\frac{k}{\epsilon}(G_{ijk}+C_{s2}(G_{ill}\delta_{jk}+G_{jll}\delta_{ik}+G_{kll}\delta_{ij}))$
Lumley (Ref. 18) (D^p_{ij})	$-\overline{pu_i}/\rho=P_D\,\overline{u_i u_l u_l}$

$$G_{ijk}=\overline{u_i u_l}\,\frac{\partial\overline{u_j u_k}}{\partial x_l}+\overline{u_j u_l}\,\frac{\partial\overline{u_i u_k}}{\partial x_l}+\overline{u_k u_l}\,\frac{\partial\overline{u_i u_j}}{\partial x_l}$$

duced at the source is assumed to be axisymmetric about the z axis and then—in the absence of mean shear—the Reynolds shear stresses are zero and $\overline{u^2}$ equals $\overline{v^2}$ throughout the contaminated region at any time. The relevant Reynolds-stress equations can, therefore, be written in the form

$$\frac{\partial\overline{u^2}}{\partial t}=\frac{\partial}{\partial z}(-\overline{wu^2})+\pi_{11}-\frac{2}{3}\epsilon, \tag{1}$$

$$\frac{\partial\overline{w^2}}{\partial t}=\frac{\partial}{\partial z}\left(-\overline{w^3}-\frac{2}{\rho}\overline{pw}\right)+\pi_{33}-\frac{2}{3}\epsilon, \tag{2}$$

where Lumley's rearrangement has been used to obtain a single, traceless, return-to-isotropy term ($\pi_{ij}=\Pi_{ij}-\epsilon_{ij}+2/3\,\epsilon\,\delta_{ij}$). In order to obtain a closed set of equations, one needs to model the turbulent-diffusion, return-to-isotropy and dissipation terms in Eqs. (1) and (2). The diffusion models used here[15–18] are defined in Table II. Pressure diffusion is specifically modeled in Lumley's scheme;[18] for all the other schemes, it is either neglected or lumped with diffusion by velocity fluctuations in a unique gradient-diffusion term. Considering the return-to-isotropy term, it will be shown that our results are independent of the selected scheme, so that we can proceed with the linear Rotta model[19]

$$\pi_{ij}=-C_1\,\epsilon\left(\frac{\overline{u_i u_j}}{k}-\frac{2}{3}\delta_{ij}\right),$$

where k is the turbulent kinetic energy ($k=\overline{u_i u_i}/2$). Finally, we use a standard transport equation to close the problem for dissipation. It takes the form

$$\frac{\partial\epsilon}{\partial t}=\frac{\partial}{\partial z}\left(C_\epsilon\overline{w^2}\frac{k}{\epsilon}\frac{\partial\epsilon}{\partial z}\right)-C_{\epsilon2}\frac{\epsilon^2}{k}. \tag{3}$$

In Ref. 20, we used this equation with all the Reynolds-stress diffusion models. In fact, it seems more consistent to use the following ''isotropic'' form with the Mellor–Herring model:[17]

$$\frac{\partial\epsilon}{\partial t}=\frac{\partial}{\partial z}\left(C_\epsilon\frac{k^2}{\epsilon}\frac{\partial\epsilon}{\partial z}\right)-C_{\epsilon2}\frac{\epsilon^2}{k}. \tag{4}$$

A. Analysis

The problem is now closed, and we shall investigate its possible solutions in the half space $z>0$. The turbulent kinetic energy can be used instead of $\overline{u^2}$, so that we proceed with the model equations for k, $\overline{w^2}$, and ϵ with the following initial and boundary conditions:

(i) for all $z>0$,
$k(z,0)=0$, $\overline{w^2}(z,0)=0$, and $\epsilon(z,0)=0$;

TABLE III. Diffusion fluxes in the turbulent-kinetic-energy and $\overline{w^2}$ equations (F and F_{33}, respectively) according to the different closure schemes studied, in the absence of mean shear.

	F	F_{33}
Daly–Harlow (Ref. 15)	$C_s\frac{k}{\epsilon}\overline{w^2}\frac{\partial k}{\partial z}$	$C_s\frac{k}{\epsilon}\overline{w^2}\frac{\partial\overline{w^2}}{\partial z}$
Hanjalić–Launder (Ref. 16)	$C_s\frac{k}{\epsilon}\overline{w^2}\left(\frac{\partial\overline{w^2}}{\partial z}+\frac{\partial k}{\partial z}\right)$	$3\,C_s\frac{k}{\epsilon}\overline{w^2}\frac{\partial\overline{w^2}}{\partial z}$
Mellor–Herring (Ref. 17)	$C_s\frac{k^2}{\epsilon}\left(\frac{\partial\overline{w^2}}{\partial z}+\frac{\partial k}{\partial z}\right)$	$3\,C_s\frac{k^2}{\epsilon}\frac{\partial\overline{w^2}}{\partial z}$
Lumley (Ref. 18)	$C_{s1}\frac{k}{\epsilon}\overline{w^2}\left(\frac{\partial\overline{w^2}}{\partial z}+\frac{\partial k}{\partial z}\right)\times(1-2\,P_D)(1+5\,C_{s2})$	$C_{s1}\frac{k}{\epsilon}\overline{w^2}\left[3\frac{\partial\overline{w^2}}{\partial z}+\left(\frac{\partial\overline{w^2}}{\partial z}+\frac{\partial k}{\partial z}\right)\times(2\,C_{s2}(3-10\,P_D)-4\,P_D)\right]$

TABLE IV. Linearized diffusivity coefficients in the turbulent-kinetic-energy equation (f) and in the $\overline{w^2}$ equation (f_{33}), as functions of α_{33} with the different diffusion schemes in the absence of mean shear. For the dissipation-rate equation, we have $h(\alpha_{33})=C_\epsilon\alpha_{33}$ for all models except Mellor–Herring, for which we use the isotropic form (4) and obtain $h(\alpha_{33})=C_\epsilon$.

	$f(\alpha_{33})$	$f_{33}(\alpha_{33})$
Daly–Harlow (Ref. 15)	$C_s\,\alpha_{33}$	$C_s\,\alpha_{33}$
Hanjalić–Launder (Ref. 16)	$C_s\,\alpha_{33}(\alpha_{33}+1)$	$3\,C_s\,\alpha_{33}$
Mellor–Herring (Ref. 17)	$C_s(\alpha_{33}+1)$	$3\,C_s$
Lumley (Ref. 18)	$C_{s1}\,\alpha_{33}(\alpha_{33}+1)\times(1-2\,P_D)(1+5\,C_{s2})$	$C_{s1}[3\,\alpha_{33}+(2\,C_{s2}(3-10\,P_D)-4\,P_D)(\alpha_{33}+1)]$

(ii) for all $t\geqslant 0$,

$$k(0,t)=k_0,\quad \overline{w^2}(0,t)=w_0^2,\quad \epsilon(0,t)=\epsilon_0,$$

$$\lim_{z\to\infty}k(z,t)=0,\quad \lim_{z\to\infty}\overline{w^2}(z,t)=0,\quad \text{and}\quad \lim_{z\to\infty}\epsilon(z,t)=0,$$

where w_0^2/k_0 sets the anisotropy level of the source. For each of the closure schemes considered here, the modeled expressions of the diffusion fluxes $F=-(\overline{u_iu_iw}/2+\overline{pw}/\rho)$ and $F_{33}=-(\overline{w^3}+2\,\overline{pw}/\rho)$ in the turbulent-kinetic-energy and $\overline{w^2}$ equations, respectively, are given in Table III.

As in the case of one- and two-equation eddy-viscosity models,[5,6] the analysis is based on the following assumptions:

(a1) the solution is of propagative (possibly weak) character in the vicinity of a front that travels along z with a finite velocity c;

(a2) the budget of the turbulent-kinetic-energy and dissipation-rate equations reduce to balances between time rate of change and turbulent diffusion in the vicinity of the front.

Recall that these assumptions apply to the model problem; in real life, (a1) should hold if the irrotational fluctuations are excluded from the statistics while (a2) may be restricted to the turbulent-kinetic-energy budget: The behavior of the *real* dissipation rate at free-stream edges remains open to question.

Coming back to the model problem, we cannot proceed at second-order closure level without linearizing the diffusion fluxes in the transport equations. To this end, we introduce the structural parameters $\alpha_{ij}=\overline{u_iu_j}/k$, noting that their values should indeed be always finite (in the range $[0,2]$ if $i=j$ and $[-1,1]$ otherwise). Then, if α_{33} is nonzero at the front and sufficiently differentiable for smaller z, its expansion, limited to zeroth order in z, can be used to write linearized forms of the k and ϵ equations there

$$\frac{\partial k}{\partial t}=\frac{\partial}{\partial z}\left(f(a_{33})\frac{k^2}{\epsilon}\frac{\partial k}{\partial z}\right)-\epsilon, \tag{5}$$

$$\frac{\partial \epsilon}{\partial t}=\frac{\partial}{\partial z}\left(h(a_{33})\frac{k^2}{\epsilon}\frac{\partial \epsilon}{\partial z}\right)-C_{\epsilon 2}\frac{\epsilon^2}{k}, \tag{6}$$

where a_{33} is the value of α_{33} at the front, and f and h are linearized diffusivity coefficients given in Table IV as functions of α_{33} for the different diffusion models. According to assumption (a2), we have to find solutions to these equations *without their destruction terms*. In these conditions, it is easily seen that the following expressions are appropriate on both sides of the front:

$$k=\mathcal{K}\,\mathrm{H}(ct-z)\left|\frac{ct-z}{\mathcal{K}^{3/2}/\mathcal{E}}\right|^m, \tag{7}$$

$$\epsilon=\mathcal{E}\,\mathrm{H}(ct-z)\left|\frac{ct-z}{\mathcal{K}^{3/2}/\mathcal{E}}\right|^n, \tag{8}$$

with

$$c=\mathcal{K}^{1/2}\frac{f(a_{33})\,h(a_{33})}{2\,h(a_{33})-f(a_{33})},\qquad m=\frac{h(a_{33})}{2\,h(a_{33})-f(a_{33})},$$

and

$$n=\frac{f(a_{33})}{2\,h(a_{33})-f(a_{33})},$$

where H is the Heaviside function, and $\mathcal{K}$ and $\mathcal{E}$ are local characteristic scales that cannot be determined without a full solution of the problem (see Ref. 20 for such a solution in the case of a two-equation model). Then relations (7) and (8) show that the destruction terms in the k and ϵ equations can actually be neglected in the vicinity of the front, provided that

$$2\,h(a_{33})-f(a_{33})>0. \tag{9}$$

This gives a condition to be satisfied for assumption (a2) to be valid. It remains to find the condition for the $\overline{w^2}$ equation to be satisfied. With no extra assumption, this equation can be linearized in the form

$$a_{33}\frac{\partial k}{\partial t}=a_{33}\frac{\partial}{\partial z}\left(f_{33}(a_{33})\frac{k^2}{\epsilon}\frac{\partial k}{\partial z}\right)+\left(\frac{\pi_{33}}{\epsilon}-\frac{2}{3}\right)\epsilon, \tag{10}$$

where f_{33} is the corresponding linearized diffusivity coefficient (given in Table IV for the different diffusion models). The factor $(\pi_{33}/\epsilon-2/3)$ in the destruction term is always finite with Rotta's model and we have checked that this is also true with most current return-to-isotropy schemes. As a consequence, the destruction term can be neglected in Eq. (10) as soon as a_{33} is nonzero. One can, therefore, consider that Eq. (10) reduces—as does the k equation—to a balance between time rate of change and turbulent diffusion. Then, identifying the degenerated forms of Eqs. (5) and (10), one gets $f(a_{33})=f_{33}(a_{33})$.

To sum up, we shall retain the result that relations (7) and (8) can be considered as local solutions on both sides of the front if a nonzero value a_{33} exists for which

TABLE V. Results of the analysis in the absence of mean shear. $h(a_{33}) = C_\epsilon a_{33}$ for all models except Mellor–Herring for which $h(a_{33}) = C_\epsilon$.

	Possible solutions	Validity condition (9)
Daly–Harlow (Ref. 15)	• any a_{33}	$C_s < 2\,C_\epsilon$
Hanjalić–Launder (Ref. 16)	• $a_{33}=2$	$C_s < \frac{2}{3} C_\epsilon$
Mellor–Herring (Ref. 17)	• $a_{33}=2$	$C_s < \frac{2}{3} C_\epsilon$
Lumley (Ref. 18) ($P_D = 1/5$)	• $a_{33}=2/3$	$C_{s1}(1+5\,C_{s2}) < 2\,C_\epsilon$
	• $a_{33}=\dfrac{2-5\,C_{s2}}{1+5\,C_{s2}}$	$C_{s1} < \dfrac{10}{9} C_\epsilon$

(i) $f(a_{33}) = f_{33}(a_{33})$;
(ii) $2\,h(a_{33}) - f(a_{33}) > 0$.

Then, $\overline{w^2}$ can be written as

$$\overline{w^2} = a_{33}\,\mathcal{K}\,\mathrm{H}(ct-z)\left|\frac{ct-z}{\mathcal{K}^{3/2}/\mathcal{E}}\right|^m. \tag{11}$$

With Eqs. (7), (8), and (11), and some ranges of value for the diffusion constants, derivatives present in the model equations may not exist at the edge. In this case, it can be shown as in Cazalbou *et al.*[6] that the solution is of weak character and, hence, valid according to (a1).

B. Results obtained with current diffusion schemes

The analysis has been applied to the diffusion schemes presented in Table II. The main results are given in Table V. Satisfaction of the relation $f(a_{33}) = f_{33}(a_{33})$ leads to specific values of a_{33} with all models except Daly–Harlow, for which the relation is satisfied whatever the value a_{33} is. Lumley's scheme admits two solutions, the first of which corresponds to isotropy at the edge while the characteristics of the second depend on the values of the modeling constants. Lumley gives these constants as functions of the return-to-isotropy constant C_1 in the form

$$C_{s1} = \frac{1}{3\,C_1}, \quad C_{s2} = \frac{C_1 - 1}{4\,C_1 + 5}.$$

With the standard value $C_1 = 1.8$, one gets $C_{s1} = 0.185$ and $C_{s2} = 0.066$, which leads to $a_{33} = 1.26$. With accepted values of the diffusion constants ($C_s = 0.11$ for Hanjalić–Launder and Mellor–Herring, 0.22 for Daly–Harlow; C_{s1} and C_{s2} as given above; $C_\epsilon = 0.18$) all models satisfy condition (9).

With reference to the discussion given in the introduction, one sees that the anisotropy measure a_{33} is kept in reasonable bounds with the Daly–Harlow model and with the isotropic solution to Lumley's. In all other cases, the solution produces an unexpectedly high degree of anisotropy at the edge. With the Hanjalić–Launder and Mellor–Herring models, one even reaches some ''one-component limit'' that is seldom observed in practice (a reentrant corner between two solid walls or the perfectly permeable wall of Perot and Moin[21] are scarce examples involving this peculiar anisotropy state as a limit).

C. Numerical results

For each of the diffusion models considered in the preceding section, we have shown that one propagative solution at least exists, provided that some constraint on the values of the modeling constants is fulfilled. The solution cannot be considered as unique, so that one has to check its relevance in practice. In order to do so, the model equations for k, $\overline{w^2}$, and ϵ have been numerically solved (computational details are given in Appendix A) with the following initial and boundary conditions:

(i) for $t = 0$,
$k = k_e$, $\overline{w^2} = \frac{2}{3} k_e$, and $\epsilon = \epsilon_e$;
(ii) for $z = 0$,
$k = k_0$, $\overline{w^2} = w_0^2$, and $\epsilon = \epsilon_0$;
(iii) for $z = H$,
$$\frac{\partial k}{\partial z} = \frac{\partial \overline{w^2}}{\partial z} = \frac{\partial \epsilon}{\partial z} = 0,$$

where H is the size of the computational domain. Note that, from a numerical point of view, it is not possible to use genuinely zero values in the undisturbed fluid, so that k_e and ϵ_e are nonzero but small compared to k_0 and ϵ_0 (typically 10^{-12} times lower). Also, to simplify the interpretation of the results, w_0^2/k_0 can be specified so that the anisotropy level of the source matches the equilibrium achieved far from the source in the model problem of steady diffusive turbulence: The equilibrium values obtained in this situation with various combinations of diffusion and return-to-isotropy models are given in Refs. 20 and 22. We shall now present the results obtained with the different diffusion schemes except Mellor–Herring, for which the results are essentially similar to those obtained with Hanjalić–Launder.

1. Hanjalić–Launder model

w_0/k_0^2 is taken equal to 1.21, which is characteristic of the equilibrium state reached in steady diffusive turbulence with this model when combined with Rotta's return-to-isotropy model. The computations have been performed with the most widely used values of the model constants, that is

$$C_s = 0.11, \quad C_1 = 1.8, \quad C_\epsilon = 0.18, \text{ and } C_{\epsilon 2} = 1.92. \tag{12}$$

As mentioned above, condition (9) is fulfilled with these values, so that the propagative solutions are likely to occur. Figures 1 and 2 show the computed turbulent viscosity ($\nu_t = k^2/\epsilon$) normalized by its value at the source (ν_{t0}) and parameter α_{33}, as functions of z/l_0 ($l_0 = k_0^{3/2}/\epsilon_0$) at three different times. One can notice:

(i) the presence of discontinuities (on the *slope* of the turbulent-viscosity profile and on the *value* of α_{33}) moving away from the source with increasing time;
(ii) the linear behavior of the turbulent-viscosity profile on the left of the discontinuity;
(iii) the limiting value $a_{33} = 2$ actually reached at the edge.

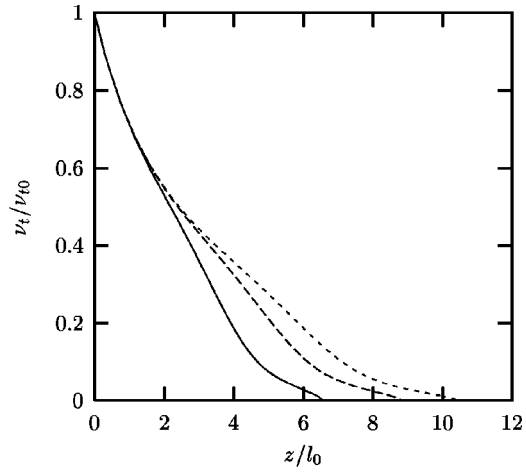

FIG. 1. Turbulence propagating from a steady plane source. Numerical result obtained with the Hanjalić–Launder model for the turbulent viscosity (k^2/ϵ) at three different times: —, $t\,\epsilon_0/k_0=20$; – –, $t\,\epsilon_0/k_0=40$; - - -, $t\,\epsilon_0/k_0=60$.

This indicates without any ambiguity the occurrence of the solution identified in the analysis. For two-equation eddy-viscosity models, it was shown by Cazalbou *et al.*[6] that such solutions were computationally well behaved with respect to the practical requirement of nonzero free-stream boundary conditions. In order to assess this point in the context of Reynolds-stress-transport modeling, sensitivity tests have been carried out with the same values of the model constants as given above, except for the value of C_ϵ, which has been lowered to 0.14 so as to violate condition (9). With this set of constants, as well as set (12), three different cases of free-stream boundary conditions have been used:

(1) A reference case with $k_e/k_0=10^{-12}$ and $\epsilon_e/\epsilon_0=10^{-12}$;
(2) a case of increased free-stream values with $k_e/k_0=10^{-6}$ and $\epsilon_e/\epsilon_0=10^{-6}$;
(3) a case of high free-stream turbulent viscosity with $k_e/k_0=10^{-6}$ and $\epsilon_e/\epsilon_0=10^{-12}$.

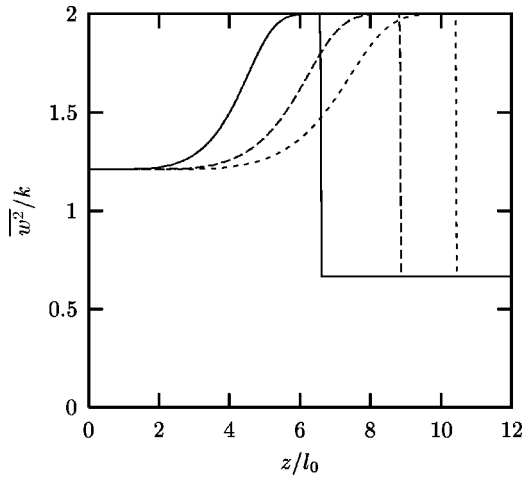

FIG. 2. Turbulence propagating from a steady plane source. Numerical result obtained with Hanjalić–Launder model for $\overline{w^2}/k$ at three different times: —, $t\,\epsilon_0/k_0=20$; – –, $t\,\epsilon_0/k_0=40$; - -, $t\,\epsilon_0/k_0=60$.

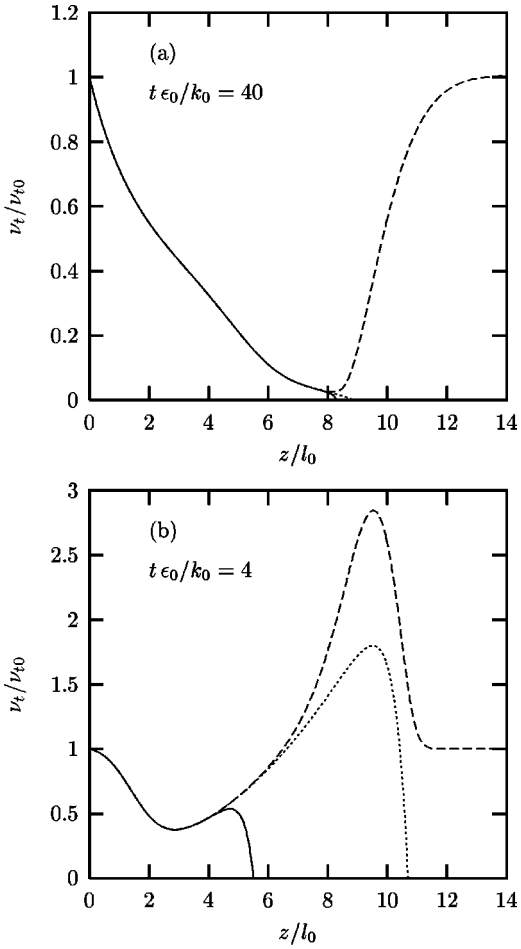

FIG. 3. Sensitivity to free-stream conditions in the case of turbulence propagating from a steady plane source, with the Hanjalić–Launder model. (a) Turbulent-viscosity profiles obtained with a set of model constants satisfying condition (9) at $t\,\epsilon_0/k_0=40$; (b) turbulent-viscosity profiles obtained with a set of model constants violating condition (9) at $t\,\epsilon_0/k_0=4$. - -, case 1; —, case 2; – –, case 3.

In the latter case, small values of the transported variables resulting in a high level of free-stream turbulent viscosity are not really inconsistent: It was argued in Ref. 6 that the value of the free-stream turbulent viscosity should indeed remain finite, but was to be considered as undefined rather than zero. The profiles of this quantity computed in the three cases are plotted in Fig. 3(a) for the original set of constants, and in Fig. 3(b) for the modified set. Predicted turbulence diffuses much faster with the latter, so that the results have not been plotted at the same time in the two figures. This, however, does not impair the comparison to be made here. It is apparent in Fig. 3(a) that, as long as the free-stream values of the transported variables are small, and irrespective of the corresponding level of turbulent viscosity, the profile of this quantity is unchanged across the turbulent region except for a very limited region in the vicinity of the front. On the other hand, when condition (9) is violated, one can see in Fig. 3(b) that the computed flow is extremely dependent on the free-stream values: The spreading of turbulence as well as the turbulent-viscosity profile are affected. Note that the free-

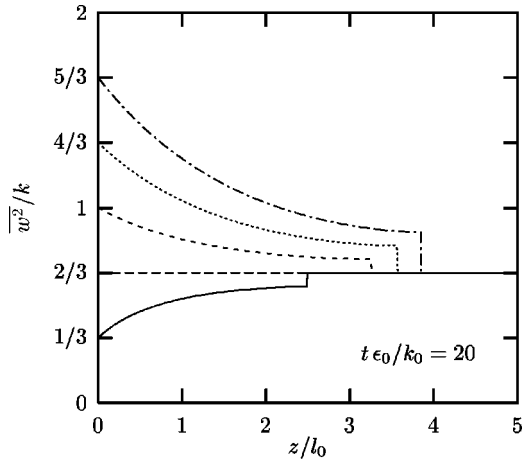

FIG. 4. Turbulence propagating from a steady plane source. Numerical result obtained for $\overline{w^2}/k$ at a given time with the Daly–Harlow model and different anisotropy levels at the source ($w_0^2/k_0 = 1/3,2/3,1,4/3,5/3$).

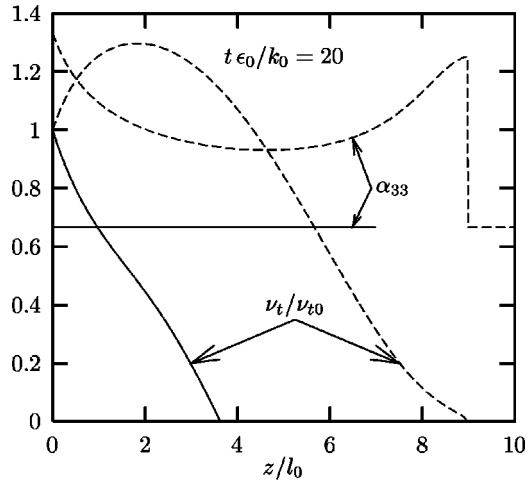

FIG. 6. Turbulence propagating from a steady plane source. Numerical results obtained at $t\,\epsilon_0/k_0 = 20$ with Lumley's model and different anisotropy levels at the source. —, $w_0^2/k_0 = 2/3$; – –, $w_0^2/k_0 = 4/3$.

stream values used in cases 1 and 2 are usually considered as reasonable choices for practical calculations, but lead here to unacceptable differences in the predictions.

2. Daly–Harlow model

For this model, the analysis shows that the propagative solution exists, and does not impose a specific level of anisotropy at the edge. The calculations have been performed with the following values of the model constants:

$$C_s = 0.22, \quad C_1 = 1.8, \quad C_\epsilon = 0.18, \text{ and } C_{\epsilon 2} = 1.92,$$

satisfying condition (9). The solution always appears, we have plotted in Fig. 4 the computed profiles of α_{33} at $t\,\epsilon_0/k_0 = 20$ for different anisotropy levels at the source. One can observe that a_{33} varies with anisotropy without questioning the propagative character of the solution. It can also be seen in Fig. 5 that, with a given anisotropy level at the source, a_{33} varies during propagation. The trend—in space and time—is always toward isotropy. Note that, for this model, isotropy is the equilibrium state in steady diffusive turbulence, and a fully isotropic solution ($\alpha_{33} = 2/3$ for all z and t) exists when the source is isotropic.

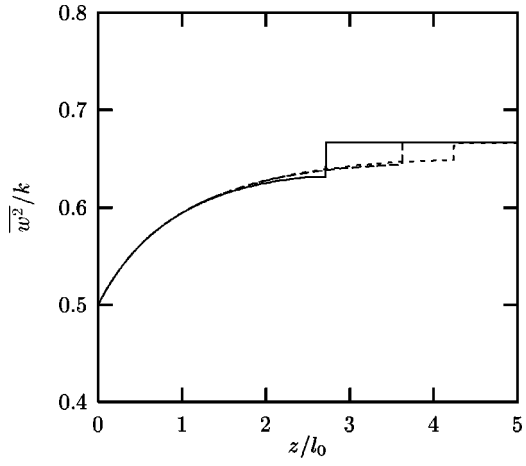

FIG. 5. Turbulence propagating from a steady plane source. Numerical result obtained for $\overline{w^2}/k$ at different times with the Daly–Harlow model and $w_0^2/k_0 = 0.5$. —, $t\,\epsilon_0/k_0 = 20$; – –, $t\,\epsilon_0/k_0 = 40$; - -, $t\,\epsilon_0/k_0 = 60$.

3. Lumley's model

With this model, the analysis shows that two different solutions exist. The first solution corresponds to isotropy at the edge and the second to a significant departure from isotropy there, with $a_{33} = 1.26$. Both solutions appear unambiguously in our calculations with an appropriate choice of w_0^2/k_0. If the source is isotropic, we get a fully isotropic solution with $\alpha_{33} = 2/3$ for all z and t (note that isotropy is also the equilibrium state in steady diffusive turbulence with this model[20,22]). When the source significantly favors $\overline{w^2}$, we get the second solution. This is apparent in Fig. 6, where α_{33} and ν_t have been plotted against z at a given time. To get the anisotropic solution, w_0^2/k_0 has been set to 4/3, and one can observe that α_{33} begins to relax toward isotropy before increasing so as to reach 1.26 at the edge. The picture is less clear when w_0^2/k_0 is lower than, or close to, 2/3. To illustrate this, numerical results obtained with the source slightly shifted from isotropy ($w_0^2/k_0 = 0.62$ and 0.71) are reported in Fig. 7. For w_0^2/k_0 slightly above 2/3, α_{33} remains roughly constant across most of the turbulent region, then exhibits a steep rise near the edge. One may think that, with a better resolution, the computed value should reach 1.26 there. When w_0^2/k_0 is slightly below 2/3, one can observe a reversed picture: α_{33} experiences a sharp decrease near the edge. In this case, the absence of a theoretical solution—with the linearization process used here—for which a_{33} would be lower than 2/3 prevents drawing any conclusion about a definite anisotropy state being reached at the edge. For even lower w_0^2/k_0, the computation quickly breaks down with negative values of $\overline{w^2}$ near the edge. At this point, we can tentatively explain this behavior by noting that, as α_{33} decreases, the linearized diffusivity of $\overline{w^2}$ can become negative [as soon as $\alpha_{33} < (4-10C_{s2})/(11+10C_{s2}) = 0.286$, see Table III], so that the model can become ''anti-diffusive'' and

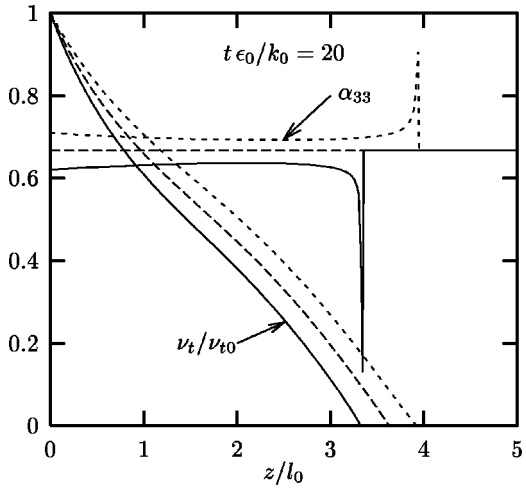

FIG. 7. Turbulence propagating from a steady plane source. Numerical results obtained at $t\,\epsilon_0/k_0=20$ with Lumley's model. The source is either isotropic: – –, $w_0^2/k_0=2/3$; or slightly shifted from isotropy: —, $w_0^2/k_0=0.62$; - - -, $w_0^2/k_0=0.71$.

experience realizability problems if the transported variable must go to zero at some location. In another respect, the calculations presented here seem to indicate that the isotropic solution is unstable, a proof is given in Appendix B showing that this is actually the case with some kind of small perturbation.

III. TIME-EVOLVING SHEAR FLOWS

The analysis can be extended to account for the effect of simple shear. This will be exemplified through the case of the time-evolving mixing layer, but the results are by no means restricted to this configuration and should apply equally to other simple-shear time-evolving flows such as jets and wakes. In the mixing-layer problem, we shall consider that at some initial time the half space $z>0$ is at rest, while the fluid filling the half space $z<0$ has a uniform velocity $2\,U_0$ along x. The analysis is performed once the shear layer has become fully turbulent. At any time in this regime, the flow is statistically homogeneous in all the planes perpendicular to z, the mean velocity remains aligned with x, and the only nonzero shear stress is $\overline{uw}$. The problem is, therefore, governed by the mean-momentum equation and the Reynolds-stress equations supplemented by their production terms ($P_{ij}=-\overline{u_iu_k}\,\partial\overline{U_j}/\partial x_k-\overline{u_ju_k}\,\partial\overline{U_i}/\partial x_k$), that is

$$\frac{\partial\overline{U}}{\partial t}=\frac{\partial}{\partial z}(-\overline{uw}), \tag{13}$$

$$\frac{\partial\overline{u^2}}{\partial t}=\frac{\partial}{\partial z}(-\overline{wu^2})-2\,\overline{uw}\frac{\partial\overline{U}}{\partial z}+\pi_{11}-\frac{2}{3}\epsilon, \tag{14}$$

$$\frac{\partial\overline{v^2}}{\partial t}=\frac{\partial}{\partial z}(-\overline{wv^2})+\pi_{22}-\frac{2}{3}\epsilon, \tag{15}$$

$$\frac{\partial\overline{w^2}}{\partial t}=\frac{\partial}{\partial z}\left(-\overline{w^3}-\frac{2}{\rho}\overline{pw}\right)+\pi_{33}-\frac{2}{3}\epsilon, \tag{16}$$

$$\frac{\partial\overline{uw}}{\partial t}=\frac{\partial}{\partial z}\left(-\overline{uw^2}-\frac{1}{\rho}\overline{pu}\right)-\overline{w^2}\frac{\partial\overline{U}}{\partial z}+\pi_{13}. \tag{17}$$

To close the problem, we still need an equation for the dissipation rate and a model for π_{ij}. The dissipation-rate equation is obtained by adding a conventional production term of the form $C_{\epsilon1}\,\epsilon/k\,P_k$ (with $P_k=P_{ii}/2$) to Eq. (3) or Eq. (4). Considering π_{ij}, one has to account for the influence of the mean motion through the "fast" pressure-strain correlation. Here again, the results will not depend on the model chosen for this term, so that we can proceed with the simple IP (isotropization of production) model. The full term is, therefore, written as

$$\pi_{ij}=-C_1\,\epsilon\left(\frac{\overline{u_iu_j}}{k}-\frac{2}{3}\delta_{ij}\right)-C_2\left(P_{ij}-\frac{2}{3}P_k\,\delta_{ij}\right).$$

The "standard" value of C_2 is 0.6. With the expressions of the fluxes given in Table VI for the different turbulent-diffusion schemes, the model problem is closed.

A. Analysis

The analysis is a simple generalization of that given in Sec. II A. We still prefer to use the equation for the turbulent kinetic energy; here, it will be used instead of the $\overline{v^2}$ equation. We start with assumptions (a1) and (a2) and look for solutions with the following linearized forms of the k and ϵ equations:

$$\frac{\partial k}{\partial t}=\frac{\partial}{\partial z}\left(f\frac{k^2}{\epsilon}\frac{\partial k}{\partial z}\right)-\overline{uw}\frac{\partial\overline{U}}{\partial z}-\epsilon, \tag{18}$$

$$\frac{\partial\epsilon}{\partial t}=\frac{\partial}{\partial z}\left(h\frac{k^2}{\epsilon}\frac{\partial\epsilon}{\partial z}\right)-C_{\epsilon1}\frac{\epsilon}{k}\,\overline{uw}\,\frac{\partial\overline{U}}{\partial z}-C_{\epsilon2}\frac{\epsilon^2}{k}. \tag{19}$$

The diffusivity coefficients f and h may now depend on both α_{13} and α_{33} (see Table VII). Consequently, Eqs. (18) and (19) will generally be valid if these parameters are nonzero at the edge and sufficiently differentiable for smaller z. Then, if a propagative solution exists, it necessarily takes the form of (7) and (8) with

$$c=\mathcal{K}^{1/2}f_E\,h_E/(2\,h_E-f_E),\quad m=h_E/(2\,h_E-f_E),$$

and $n=f_E/(2\,h_E-f_E)$,

where $f_E=f(a_{33},a_{13})$, $h_E=h(a_{33},a_{13})$; a_{13} being the value of α_{13} at the edge. For the same reason as above, the dissipation and return-to-isotropy terms can be neglected as soon as $2\,h_E-f_E>0$. Noting that $\overline{uw}$ and $\overline{U}$ behave in the same way at the edge (according to the momentum equation), and that $\overline{uw}=a_{13}k$ to leading order, relations (7) and (8) can be used to show that the production term and the fast pressure-strain correlation are also negligible in the vicinity of the edge. This shows that the budget of the turbulent-kinetic-energy and dissipation-rate equations actually reduce to balances between time rate of change and diffusion, so that assumption (a2) is valid.

In order to check that the three remaining Reynolds-stress equations can be locally satisfied, one can linearize them in the form

TABLE VI. Diffusion fluxes in the turbulent-kinetic-energy equation (F) and in the Reynolds-stress equations (F_{ij}) according to the different closure schemes studied in time-evolving shear flows.

Daly–Harlow (Ref. 15)	$F=C_s\frac{k}{\epsilon}\overline{w^2}\frac{\partial k}{\partial z}$
	$F_{11}=C_s\frac{k}{\epsilon}\overline{w^2}\frac{\partial \overline{u^2}}{\partial z}$
	$F_{33}=C_s\frac{k}{\epsilon}\overline{w^2}\frac{\partial \overline{w^2}}{\partial z}$
	$F_{13}=C_s\frac{k}{\epsilon}\overline{w^2}\frac{\partial \overline{uw}}{\partial z}$
Hanjalić–Launder (Ref. 16)	$F=C_s\frac{k}{\epsilon}\left(\overline{w^2}\frac{\partial k}{\partial z}+\overline{w^2}\frac{\partial \overline{w^2}}{\partial z}+\overline{uw}\frac{\partial \overline{uw}}{\partial z}\right)$
	$F_{11}=C_s\frac{k}{\epsilon}\left(\overline{w^2}\frac{\partial \overline{u^2}}{\partial z}+2\,\overline{uw}\frac{\partial \overline{uw}}{\partial z}\right)$
	$F_{33}=3\,C_s\frac{k}{\epsilon}\overline{w^2}\frac{\partial \overline{w^2}}{\partial z}$
	$F_{13}=C_s\frac{k}{\epsilon}\left(\overline{uw}\frac{\partial \overline{w^2}}{\partial z}+2\,\overline{w^2}\frac{\partial \overline{uw}}{\partial z}\right)$
Mellor–Herring (Ref. 17)	$F=C_s\frac{k^2}{\epsilon}\left(\frac{\partial k}{\partial z}+\frac{\partial \overline{w^2}}{\partial z}\right)$
	$F_{11}=C_s\frac{k^2}{\epsilon}\frac{\partial \overline{u^2}}{\partial z}$
	$F_{33}=3\,C_s\frac{k^2}{\epsilon}\frac{\partial \overline{w^2}}{\partial z}$
	$F_{13}=2\,C_s\frac{k^2}{\epsilon}\frac{\partial \overline{uw}}{\partial z}$
Lumley (Ref. 18)	$F=C_{s1}\frac{k}{\epsilon}(1+5\,C_{s2})(1-2\,P_D)\left(\overline{w^2}\frac{\partial k}{\partial z}+\overline{w^2}\frac{\partial \overline{w^2}}{\partial z}+\overline{uw}\frac{\partial \overline{uw}}{\partial z}\right)$
	$F_{11}=C_{s1}\frac{k}{\epsilon}\left(2\,C_{s2}\,\overline{w^2}\frac{\partial k}{\partial z}+\overline{w^2}\frac{\partial \overline{u^2}}{\partial z}+2\,C_{s2}\,\overline{w^2}\frac{\partial \overline{w^2}}{\partial z}+2(1+C_{s2})\,\overline{uw}\frac{\partial \overline{uw}}{\partial z}\right)$
	$F_{33}=3\,C_{s1}\frac{k}{\epsilon}\left(2\,C_{s2}\,\overline{w^2}\frac{\partial k}{\partial z}+(1+2\,C_{s2})\,\overline{w^2}\frac{\partial \overline{w^2}}{\partial z}+2\,C_{s2}\,\overline{uw}\frac{\partial \overline{uw}}{\partial z}\right)$
	$-4\,P_D\,C_{s1}\frac{k}{\epsilon}(1+5\,C_{s2})\left(\overline{w^2}\frac{\partial k}{\partial z}+\overline{w^2}\frac{\partial \overline{w^2}}{\partial z}+\overline{uw}\frac{\partial \overline{uw}}{\partial z}\right)$
	$F_{13}=C_{s1}\frac{k}{\epsilon}\left(2\,C_{s2}\,\overline{uw}\frac{\partial k}{\partial z}+2\,C_{s2}\,\overline{uw}\frac{\partial \overline{u^2}}{\partial z}+\overline{uw}\frac{\partial \overline{w^2}}{\partial z}+2(1+C_{s2})\,\overline{w^2}\frac{\partial \overline{uw}}{\partial z}\right)$
	$-2\,P_D\,C_{s1}\frac{k}{\epsilon}(1+5\,C_{s2})\left(\overline{uw}\frac{\partial k}{\partial z}+\overline{uw}\frac{\partial \overline{u^2}}{\partial z}+\overline{w^2}\frac{\partial \overline{uw}}{\partial z}\right)$

TABLE VII. Linearized diffusivity coefficients in the Reynolds-stress and turbulent-kinetic-energy equations as functions of α_{11}, α_{33}, and α_{13} with the different diffusion schemes in time-evolving shear flows. For the dissipation-rate equation, we still have $h(\alpha_{33})=C_\epsilon\,\alpha_{33}$ for all models except Mellor–Herring, for which $h(\alpha_{33})=C_\epsilon$.

Daly–Harlow (Ref. 15)	$f=f_{11}=f_{33}=f_{13}=C_s\,\alpha_{33}$
Hanjalić–Launder (Ref. 16)	$f=C_s(\alpha_{33}+\alpha_{33}^2+\alpha_{13}^2)$
	$f_{11}=C_s(\alpha_{33}+2\,\alpha_{13}^2/\alpha_{11})$
	$f_{33}=f_{13}=3\,C_s\,\alpha_{33}$
Mellor–Herring (Ref. 17)	$f=C_s(1+\alpha_{33})$
	$f_{11}=f_{33}/3=f_{13}/2=C_s$
Lumley (Ref. 18)	$f=C_{s1}(1+5\,C_{s2})(1-2\,P_D)(\alpha_{33}+\alpha_{33}^2+\alpha_{13}^2)$
	$f_{11}=C_{s1}[\alpha_{33}+2\,\alpha_{13}^2/\alpha_{11}+2\,C_{s2}(\alpha_{33}+\alpha_{33}^2+\alpha_{13}^2)/\alpha_{11}]$
	$f_{33}=C_{s1}[3\,\alpha_{33}+2\,(C_{s2}(3-10\,P_D)-2\,P_D)(\alpha_{33}+\alpha_{33}^2+\alpha_{13}^2)/\alpha_{33}]$
	$f_{13}=C_{s1}[3\,\alpha_{33}+2\,(1+\alpha_{11}+\alpha_{33})(C_{s2}(1-5\,P_D)-P_D)]$

TABLE VIII. Results of the analysis for time-evolving shear flows. $h(a_{33})=C_\epsilon a_{33}$ for all models except Mellor–Herring for which $h(a_{33})=C_\epsilon$.

	Possible solutions	Validity condition
Daly–Harlow (Ref. 15)	• any (a_{11},a_{33},a_{13})	$C_s<2\,C_\epsilon$
Hanjalić–Launder (Ref. 16)	$\bullet a_{11}+a_{33}=2,\ a_{11}\times a_{33}=a_{13}^2$	$C_s<\frac{2}{3}C_\epsilon$
Mellor–Herring (Ref. 17)	$\bullet a_{11}=0,\ a_{33}=2,\ a_{13}=0$	$C_s<\frac{2}{3}C_\epsilon$
Lumley (Ref. 18) ($P_D=1/5$)	$\bullet a_{11}=a_{33}=2/3,\ a_{13}=0$	$C_{s1}(1+5\,C_{s2})<2\,C_\epsilon$
	$\bullet a_{11}=\dfrac{15\,C_{s2}}{2(1+5\,C_{s2})},\quad a_{33}=\dfrac{2-5\,C_{s2}}{1+5\,C_{s2}},\quad a_{13}=0$	$C_{s1}<\dfrac{10}{9}C_\epsilon$
	$\bullet a_{11}=0,\quad a_{33}=\dfrac{2-5\,C_{s2}}{1+5\,C_{s2}},\quad a_{13}=0$	$C_{s1}<\dfrac{10}{9}C_\epsilon$

$$\frac{\partial\overline{u^2}}{\partial t}=\frac{\partial}{\partial z}\left(f_{11}\frac{k^2}{\epsilon}\frac{\partial\overline{u^2}}{\partial z}\right)-2\,\overline{uw}\frac{\partial\overline{U}}{\partial z}+\left(\frac{\pi_{11}}{\epsilon}-\frac{2}{3}\right)\epsilon, \tag{20}$$

$$\frac{\partial\overline{w^2}}{\partial t}=\frac{\partial}{\partial z}\left(f_{33}\frac{k^2}{\epsilon}\frac{\partial\overline{w^2}}{\partial z}\right)+\left(\frac{\pi_{33}}{\epsilon}-\frac{2}{3}\right)\epsilon, \tag{21}$$

$$\frac{\partial\overline{uw}}{\partial t}=\frac{\partial}{\partial z}\left(f_{13}\frac{k^2}{\epsilon}\frac{\partial\overline{uw}}{\partial z}\right)-\overline{w^2}\frac{\partial\overline{U}}{\partial z}+\pi_{13}, \tag{22}$$

with the appropriate restrictions on the behavior of α_{11}, α_{33}, and α_{13}. If a_{ij} is nonzero, it can be readily shown that the budget of $\overline{u_iu_j}$ reduces to a balance between time rate of change and diffusion, and that the value of its linearized diffusivity coefficient at the edge should be equal to f_E for the equation to be satisfied. Then the general condition for relations (7) and (8) to be local solutions in the vicinity of the edge is that

$$f_{33}(a_{33},a_{13})=f_E \text{ and } [f_{11}(a_{33},a_{13})=f_E \text{ or } a_{11}=0]$$
$$\text{and } [f_{13}(a_{33},a_{13})=f_E \text{ or } a_{13}=0]. \tag{23}$$

Note that we still consider solutions for which a_{13} or a_{11} can be zero since, for some of the models considered later:

(i) h and f do not depend on α_{13} so that expanding this parameter in powers of z is not needed;
(ii) if a_{13} or a_{11} is zero, the corresponding Reynolds stress may simply respond to the right-hand side terms of its equation without any influence on the structure of the solution, and its evolution may not necessarily result from a degenerate balance.

B. Results obtained with current diffusion schemes in the presence of mean shear

For each of the diffusion schemes, realizable sets of a_{ij} have been systematically sought in all the cases for which proposition (23) could be true. The results are given in Table VIII. The shear-free solution plus $a_{13}=0$ is indeed a possible solution for all models. Moreover, one can see that:

(i) the Daly–Harlow model still does not constrain the anisotropy state in the vicinity of the edge;
(ii) the Hanjalić–Launder model has a specific solution for which u and w are fully correlated at the edge with $a_{11}\times a_{33}=a_{13}^2$ and, therefore, $C_{uw}=1$ (C_{uw} is the correlation coefficient between u and w, defined by $\overline{uw}=C_{uw}\sqrt{\overline{u^2}}\sqrt{\overline{w^2}}$);
(iii) the Mellor–Herring model has no solution other than the shear-free solution;
(iv) the only specific solution obtained for Lumley's model is a close variant of the anisotropic shear-free solution (with the same value of a_{33}, and $a_{11}=0$ instead of $a_{11}=a_{22}=(2-a_{33})/2$).

For all models, the validity condition remains the same as in the shear-free case.

C. Numerical results for the time-evolving shear layer

The modeled forms of Eqs. (13)–(17), supplemented with the dissipation-rate equation written in appropriate form [Eq. (3) or (4)], have been numerically solved for each of the diffusion schemes considered here. The ideal initial condition with its step in the velocity profile is difficult to use with a conventional numerical method, so that we initialize the computation with an approximate finite-width shear layer such that:

(i) for $z<\delta_0$,
$$\frac{\overline{U}}{U_0}=1-\sin\left(\pi\frac{z}{2\,\delta_0}\right) \quad\text{and}\quad \frac{\overline{uw}}{U_0^2}\times 100=1+\cos\left(\pi\frac{z}{\delta_0}\right),$$
$$k=\frac{\overline{uw}}{0.3},\quad \overline{u^2}=\overline{v^2}=\overline{w^2}=\tfrac{2}{3}k,\quad\text{and}\quad \epsilon=\frac{k^{3/2}}{\delta_0};$$
(ii) for $z\geqslant\delta_0$,
$$\overline{U}=0,\quad \overline{u^2}=\overline{v^2}=\overline{w^2}=\tfrac{2}{3}k_e,\quad \overline{uw}=0.3\,k_e,$$
$$\text{and}\quad \epsilon=\epsilon_e.$$

For $t>0$, the following boundary conditions are used:

(i) for $z=0$,
$$\overline{U}=U_0,\quad \frac{\partial\overline{u^2}}{\partial z}=\frac{\partial\overline{v^2}}{\partial z}=\frac{\partial\overline{w^2}}{\partial z}=\frac{\partial\overline{uw}}{\partial z}=0,\quad\text{and}\quad \frac{\partial\epsilon}{\partial z}=0;$$
(ii) for $z=H$,

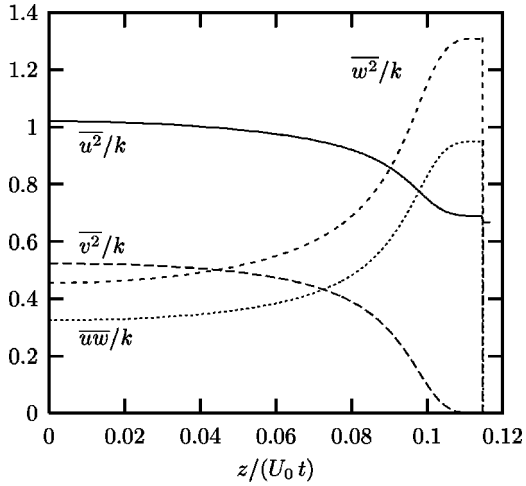

FIG. 8. Time-evolving mixing layer. Anisotropy parameters in the self-similarity regime computed with the Hanjalić–Launder model. (We show in Appendix C that $\overline{v^2}$ goes to zero like k^3 at the edge.)

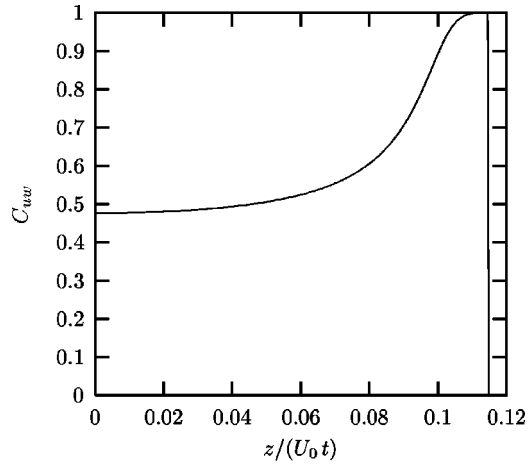

FIG. 9. Time-evolving mixing layer. C_{uw} correlation coefficient in the self-similarity regime computed with the Hanjalić–Launder model.

$$\overline{U}=0, \quad \frac{\partial \overline{u^2}}{\partial z}=\frac{\partial \overline{v^2}}{\partial z}=\frac{\partial \overline{w^2}}{\partial z}=0,$$

$$\overline{uw}=0, \text{ and } \frac{\partial \epsilon}{\partial z}=0.$$

Computations are advanced in time until self-similar solutions are reached. For all our results, the final width of the layer is more than $50\,\delta_0$, and we have checked that $\overline{U}/U_0$, $\overline{u_i u_j}/U_0^2$ and $\epsilon t/U_0$ all collapse when plotted against $z/(U_0 t)$. Results will be presented for all models except Lumley's, for which negative values of $\overline{w^2}$ quickly occur and prevent a numerical solution being obtained. This is probably because anisotropy in the core of the mixing layer being detrimental to $\overline{w^2}$, the numerical solution deviates from isotropy at the edge, to produce the low values of α_{33} which we think are responsible for realizability problems there. We shall now review the results obtained with the other diffusion models.

1. Hanjalić–Launder model

The evolution across the mixing layer of the anisotropy parameters α_{ij} and correlation coefficient C_{uw} computed with the Hanjalić–Launder model are plotted in Figs. 8 and 9. One can see that $\overline{v^2}/k$ goes to zero while C_{uw} reaches 1 at the edge: this indicates that the solution identified in the analysis is actually reached in practice. With reference to the shear-free case, the value of $\overline{w^2}/k$ in the vicinity of the edge has decreased but remains high, about 1.3; the value of the shear-stress parameter $\overline{uw}/k$ also appears to be high, slightly above 0.9 (note that these particular values are not fixed by the structure of the solution, but may vary from one shear flow to another, and with the choice of pressure-strain model). Turbulence, therefore, reaches the two-component limit at the edge, and is unrealistically correlated and efficient in a significant part of the layer: To our knowledge, values of C_{uw} and $\overline{uw}/k$ significantly higher than 0.5 and 0.3, respectively, have never been reported for *real* turbulence. We have seen above that having some α_{ij} going to zero at the edge leaves the possibility of a nondegenerate budget in the corresponding Reynolds-stress equation. This is the case here with $\overline{v^2}$, whose computed budget is compared with that of $\overline{u^2}$ in Fig. 10. The latter actually displays a balance between time rate of change and turbulent diffusion near the edge, all the other terms being negligible in this region. The figure clearly shows that this is not true of the budget of $\overline{v^2}$, for which we show in Appendix C that the sum of the pressure-strain and dissipation terms contributes exactly 1/3 of the time rate of change.

2. Daly–Harlow model

Figure 11 shows the evolution across the mixing layer of the anisotropy parameters α_{ij} computed with the Daly–Harlow model. As in the shear-free case and in agreement with the analysis, all of them reach finite nonzero values at the edge. Mild variations toward the values corresponding to isotropy for each of the parameters are exhibited across the layer, and one can consider that anisotropy at the edge mostly reflects the anisotropy state in the core of the layer.

3. Mellor–Herring model

For this model, we use the same values of the model constants as for Hanjalić–Launder model. The analysis indicates that $\overline{w^2}/k$ reaches 2 at the edge, while all the other α_{ij} go to zero there. This behavior is confirmed by the numerical results reported in Fig. 12. Here again, unrealistic turbulence is predicted near the edge: The one-component limit is reached and the shear-stress parameter $\overline{uw}/k$ peaks at 0.6 before going to zero (such high values are presumably linked with those of $\overline{w^2}/k$). The computed budgets (not shown here) also confirm an analysis similar to that given in Appendix C, which shows that having all the α_{ij} except α_{33} going to zero at the edge is obtained with nondegenerate budgets for $\overline{u^2}$ and $\overline{v^2}$, while the $\overline{uw}$ budget still exhibits the usual balance between time rate of change and diffusion.

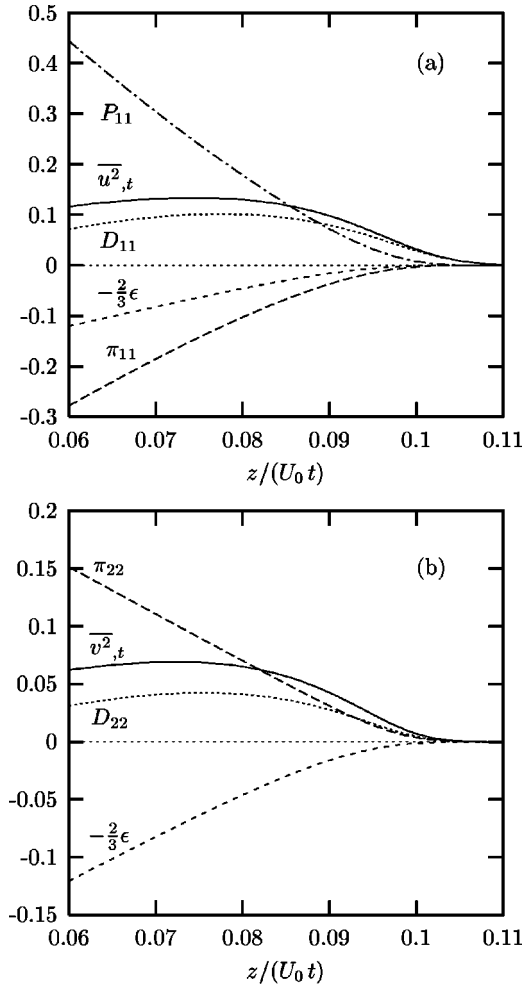

FIG. 10. Time-evolving mixing layer. $\overline{u^2}$ (a) and $\overline{v^2}$ (b) budgets computed with the Hanjalić–Launder model.

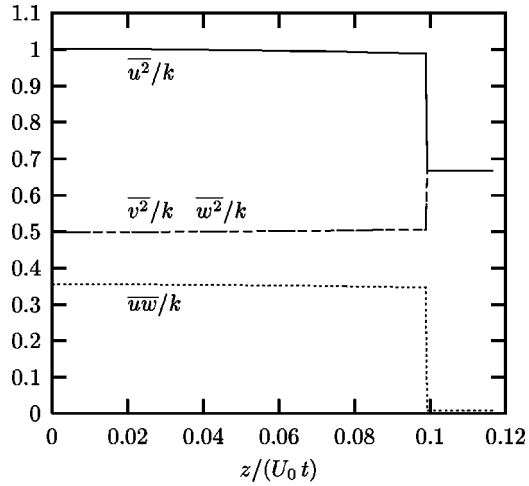

FIG. 11. Time-evolving mixing layer. Anisotropy parameters in the self-similarity regime computed with the Daly–Harlow model.

IV. REALIZABILITY OF LUMLEY'S MODEL

In this section, we shall use the results of the analysis to show how Lumley's model could be recalibrated so as to avoid the difficulties mentioned in Secs. II C and III C. Such difficulties have already been reported (see Lumley and Mansfield[23]), and we believe that they refer to the realizability question in connection with the possible anti-diffusive nature of the diffusion scheme. As a matter of fact, if pressure diffusion of turbulent kinetic energy is to be modeled with a gradient diffusion approximation, it should indeed be anti-diffusive: In free-shear flows, experiment as well as simulation show that pressure diffusion mostly acts as counter-gradient transport. Lumley's model is consistent with this and cannot be criticized from this point of view. However requiring that the global model—diffusion by pressure *and* velocity fluctuations—should not become anti-diffusive is not obviously contradicted by experiment, and the global model would probably be better behaved from mathematical and numerical points of view. The reason for such a requirement is that, unlike "natural" diffusion, anti-diffusion is not domain-invariant, i.e.: If the value of the transported variable is initially contained in a bounded domain, it will escape from this domain under the effect of diffusion alone. For an essentially positive quantity going to zero somewhere in the flow, the occurrence of negative, "unrealizable," values follows.

Modifications to Lumley's model intended to avoid such behavior in the flows investigated here are possible. Considering the shear-free case, we have indicated that the linearized diffusivity coefficient f_{33} becomes negative as soon as α_{33} becomes lower than 0.286, with the original values of the modeling constants. The expression of this coefficient given in Table IV shows that it cannot become negative in this flow if $C_{s2} \geqslant 2\,P_D/(3-10\,P_D)$. The limiting case

$$C_{s2}=\frac{2\,P_D}{3-10\,P_D}, \tag{24}$$

is sufficient and can be used to recalibrate the model. The analysis then gives the following solution at the edge:

$$a_{33}=\frac{2-8\,P_D}{1-2\,P_D} \quad \text{and} \quad a_{11}=a_{22}=1-\frac{a_{33}}{2}, \tag{25}$$

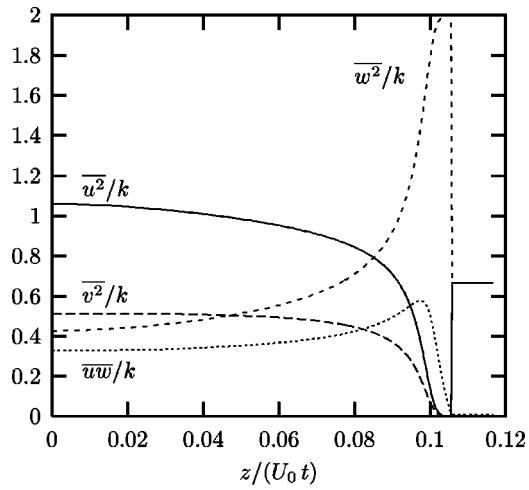

FIG. 12. Time-evolving mixing layer. Anisotropy parameters in the self-similarity regime computed with the Mellor–Herring model. (An analysis similar to that given in Appendix C shows that, at the edge, $\overline{u^2}$ and $\overline{v^2}$ go to zero like k^2, and $\overline{uw}$ like $k^{3/2}$.)

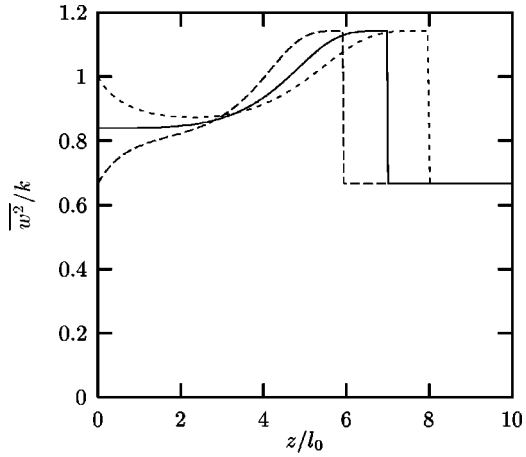

FIG. 13. Turbulence propagating from a steady plane source. $\overline{w^2}/k$ for different anisotropy levels at the source ($w_0/k_0=2/3,0.84,1$) computed with Lumley's model and a new set of constants satisfying realizability.

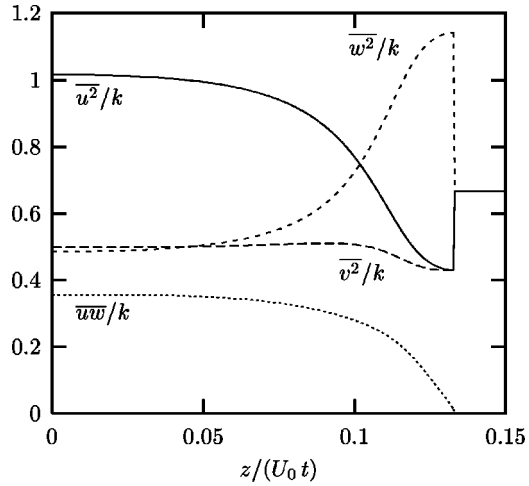

FIG. 14. Time-evolving mixing layer. Anisotropy parameters computed in the self-similarity regime with Lumley's model and a new set of constants satisfying realizability.

with the validity condition: $C_{s1}<2\,C_\epsilon/3$. It appears that Eq. (24) also ensures that f_{33} never becomes negative in the simple-shear case, for which relations (25) remain valid with $a_{13}=0$. To illustrate how the model can be recalibrated on this basis, we propose to evaluate the following set of constants:

$$C_{s1}=0.11,\quad C_\epsilon=0.18,\quad P_D=0.15,\quad C_{s2}=0.2,$$
$$C_{\epsilon 1}=1.44,\quad \text{and}\quad C_{\epsilon 2}=1.92, \tag{26}$$

satisfying relations (25) and the validity condition. With Rotta and IP schemes for the pressure-strain correlation, it can be shown using the analysis given in Ref. 20 that the following results are obtained in steady diffusive turbulence: The equilibrium value of $\overline{w^2}/k$ is 0.84, the spatial decrease in the rms value of the velocity fluctuation is proportional to $z^{-1.27}$ and the slope of the *linear* length scale equals 0.29; all of them fall into accepted experimental ranges (see Ref. 20). In propagating turbulence and simple-shear flows, relations (25) indicate that α_{33} should reach 1.14 at the edge. Calculations have been performed for turbulence propagating from a steady plane source and the time-evolving mixing layer without any of the difficulties mentioned above. The results are reported in Figs. 13 and 14, respectively. One can see in Fig. 13 that a solution in agreement with relations (25) is obtained with different anisotropy levels at the source, and that it is now obviously stable. Figure 14 shows the evolutions of the anisotropy parameters in the mixing layer. It appears that, at the edge, $\overline{uw}/k$ goes to zero, turbulence becomes axisymmetric with $\overline{u^2}/k=\overline{v^2}/k$, and $\overline{w^2}/k$ reaches 1.14 as predicted in the analysis. The growth rate of the mixing layer measured as

$$r=\frac{1}{2U_0}\frac{d\theta}{dt}\ \text{ with }\ \theta=2\int_0^\infty \frac{\overline{U}}{2U_0}\left(1-\frac{\overline{U}}{2U_0}\right)dz,$$

amounts to 1.41×10^{-2} which is at the low end of the range of experimental results ($1.4\times10^{-2}<r<2.2\times10^{-2}$, see Rogers and Moser[24]). Now, the difference in the values of the diffusion constants as given by (26) and the original theoretical estimates is disturbing. Considering the calibration of C_{s1}, diffusion of $\overline{w^2}$—the component in the direction of diffusion—is probably the most important to be assessed; one can see in Tables III and VI that using relations (25) gives an expression of Lumley's diffusion flux (F_{33}) which is the same as that obtained with the Hanjalić–Launder model, C_s being simply replaced by C_{s1}. Therefore, lowering C_{s1} to 0.11 (the well-established Hanjalić–Launder value) seems to be justified, and follows from the increase in C_{s2} resulting from the use of relations (25) with a low value of P_D. Taking P_D lower than 1/5 (the value initially recommended by Lumley[18]) is permitted: It was recognized by Shih, Lumley, and Janicka[25] that P_D was in fact a free coefficient, while Straatman *et al.*[22] later showed that a low value was needed to obtain $\overline{w^2}>\overline{u^2}$ in steady diffusive turbulence. Finally, it is interesting to note that, in an examination of simulation and experimental data, Straatman[26] has proposed a modification to Lumley's model in which the value of C_{s2} is also significantly increased (0.31), with low values of P_D (0.142–0.153) needed to account for the situation of steady diffusive turbulence. Straatman assessed the effectiveness of his modified model with computations of several flows of practical interest. The present analysis supports Straatman's proposal, showing that his modified model should be free of the realizability problems encountered in the original version.

V. SUMMARY AND CONCLUSION

The present study establishes that most turbulent-diffusion schemes used in the context of Reynolds-stress-transport modeling lead to possibly weak propagative solutions, which are similar to those previously reported in the case of eddy-viscosity models. As a consequence, these solutions exhibit the same advantages in terms of insensitivity to the free-stream conditions and physical behavior. To benefit from these advantages, some inequalities relating the modeling constants have to be satisfied, these can be established in the course of the analysis and used in the calibration

of models. The main extra piece of information brought out in the context of Reynolds-stress-transport modeling is that the propagative solution can strongly influence the prediction of anisotropy near the edge. Among the diffusion models investigated here, Daly–Harlow is the only one for which anisotropy at the edge follows from the state of the flow in the core of the layer. With all the other models, essential characteristics of anisotropy at the edge are either fully independent of it (Mellor–Herring, Hanjalić–Launder) or marginally dependent: With the original version of Lumley's model, there is a finite number of solutions at the edge, and the state of the flow in the core of the layer can only influence the selection of one of these solutions. According to our discussion in the introduction, Daly–Harlow may, therefore, be considered as the best-behaved of the models considered here.

From a practical point of view, one has to wonder about the need to predict precisely anisotropy near the edge: In this region, all the Reynolds stresses go to zero and the comparison between prediction and experiment is probably less severe when the Reynolds stresses rather than the anisotropy parameters are considered. The point is that modern pressure-strain models use the anisotropy parameters to ensure realizability in the two-component limit: The latter is expected in the vicinity of solid walls and free surfaces but certainly not at free-stream edges. Therefore, combining these schemes with Hanjalić–Launder or Mellor–Herring diffusion schemes may also cause erroneous evaluations of the redistribution processes. This is probably one of the reasons why the ''old'' Daly–Harlow scheme is still preferred by modelers in recent implementations of Reynolds-stress-transport models.

In another respect, an interesting by-product of the analysis appears to be the interpretation that can be made of difficulties encountered in computing simple-shear flows with Lumley's model. It has led us to introduce a new realizability condition, according to which the model for the whole diffusion term in the normal-Reynolds-stresses equations should not become anti-diffusive. The analysis helps to determine modified values of the model constants ensuring that it does not happen in the computation of simple shear flows. This is a necessary condition, and the need for the sufficient condition—according to which it should *never* happen—remains an open question. Also, possible implications for the diffusion of the shear stresses could be further investigated.

ACKNOWLEDGMENTS

The authors gratefully acknowledge helpful comments and suggestions from Professor P. Bradshaw, Professor J. L. Lumley, and Dr. P. R. Spalart.

APPENDIX A: NUMERICAL DETAILS

The numerical method used for solving the model problem of turbulence propagating from a steady plane source in Sec. II C, and time-evolving mixing layer in Sec. III C, is based on a time-marching procedure with finite-volume discretizations in space and time. The time discretization is first-order accurate, explicit for destruction and fully implicit for diffusion. The equations are written for the vector of the transported variables, so that implicit evaluation of the diffusion fluxes leads to the inversion of a block-tridiagonal matrix at each time step. The space discretization is conservative with a constant step. In all calculations 600 grid points are used across the computational domain, a majority of which is inside the turbulent region.

APPENDIX B: STABILITY ANALYSIS OF THE ISOTROPIC SOLUTION TO LUMLEY'S MODEL

In the problem of turbulence propagating from an *isotropic* steady plane source, Lumley's model with $P_D=1/5$ admits an isotropic solution such that $\alpha_{33}=2/3$ for all z and t inside the turbulent region. To get some insight into the stability of this solution, one can consider a perturbation in $\overline{w^2}$ at a given time t_p, such as $\alpha_{33}=2/3+\vartheta$, with ϑ constant along z. The evolution equation for α_{33} can be obtained from the combination of the k and $\overline{w^2}$ equations

$$\frac{\partial \alpha_{33}}{\partial t}=\frac{1}{k}(D_{33}-\alpha_{33}D_k)+\frac{\epsilon}{k}\left(\frac{\pi_{33}}{\epsilon}-\frac{2}{3}+\alpha_{33}\right).$$

Introducing the modeled expressions of the turbulent-diffusion and return-to-isotropy (Rotta) terms, and taking into account that $\alpha_{33}=2/3+\vartheta$, one gets

$$k\frac{\partial \alpha_{33}}{\partial t}=\vartheta(1-C_1)\times\epsilon+\left[\vartheta\left(\frac{8}{15}-\frac{10}{3}C_{s2}\right)+\vartheta^2\left(\frac{2}{5}-7\,C_{s2}\right)+\vartheta^3\left(-\frac{3}{5}-3\,C_{s2}\right)\right]\times\frac{\partial}{\partial z}\left(C_{s1}\frac{k^2}{\epsilon}\frac{\partial k}{\partial z}\right).$$

This equation is exact at $t=t_p$ since ϑ is constant in z. The term on the first line of the rhs has a stabilizing effect since $(1-C_1)$ is negative. To first order in ϑ, the term on the second line of the rhs has an opposite effect: It is proportional to the diffusion of k which is always positive in this flow, and the coefficient of proportionality is also positive when $C_{s2}=0.066$ (in fact, as soon as $C_{s2}<0.16$). This term is dominant at the edge, so that any perturbation of the type considered here is amplified in this region. Note that the same analysis applied to the Daly–Harlow model—which also admits an isotropic solution in this problem—leads to an opposite conclusion, the term on the second line of the rhs being zero to first order in ϑ.

APPENDIX C: BEHAVIOR OF $\overline{v^2}$ AT THE EDGE OF THE MIXING LAYER ACCORDING TO THE HANJALIĆ–LAUNDER MODEL

In simple-shear flows, the Hanjalić–Launder model has been shown to produce a propagative solution with $a_{22}=0$ and $a_{11}\times a_{33}=a_{13}^2$. We also have $f_E=3\,C_s\,a_{33}$ and $h_E=C_\epsilon\,a_{33}$, so that the propagation velocity c and the exponents for the turbulent kinetic energy and its dissipation rate in Eqs. (7) and (8) take the forms

$$c=\mathcal{K}^{1/2}\frac{3\,a_{33}\,C_s\,C_\epsilon}{2\,C_\epsilon-3\,C_s},\quad m=\frac{C_\epsilon}{2\,C_\epsilon-3\,C_s},$$

$$\text{and}\quad n=\frac{3\,C_s}{2\,C_\epsilon-3\,C_s}.$$

Now, the fact that a_{22} is zero leaves the possibility that the budget of $\overline{v^2}$ does not reduce to the usual balance between time rate of change and turbulent diffusion. In order to check this point, we shall specify the behavior of $\overline{v^2}$ letting

$$\overline{v^2}=\mathcal{V}^2\ \mathrm{H}(ct-z)\left|\frac{ct-z}{\mathcal{K}^{3/2}/\mathcal{E}}\right|^l, \tag{C1}$$

$$\overline{w^2}=a_{33}\mathcal{K}\ \mathrm{H}(ct-z)\left|\frac{ct-z}{\mathcal{K}^{3/2}/\mathcal{E}}\right|^m, \tag{C2}$$

$$\overline{uw}=a_{13}\mathcal{K}\ \mathrm{H}(ct-z)\left|\frac{ct-z}{\mathcal{K}^{3/2}/\mathcal{E}}\right|^m, \tag{C3}$$

$$\overline{U}=\frac{a_{13}\mathcal{K}}{c}\ \mathrm{H}(ct-z)\left|\frac{ct-z}{\mathcal{K}^{3/2}/\mathcal{E}}\right|^m. \tag{C4}$$

The $\overline{v^2}$ equation is examined in the form

$$\frac{\partial\overline{v^2}}{\partial t}-D_{22}=\pi_{22}-\frac{2}{3}\epsilon,$$

where the Rotta and IP schemes will be used to model the pressure-strain correlation. Then, using Eqs. (8), (9), (C1)–(C4), the following relations can be shown to hold in the vicinity of the edge:

$$\text{rhs}=\mathcal{E}Z^n\times\frac{2}{3}\left(C_1-1+\frac{C_2\,a_{11}}{3\,C_s}\right),$$

$$\text{lhs}=\mathcal{E}Z^{l-1}\times l\,\frac{\mathcal{V}^2}{\mathcal{K}}\,C_s\,a_{33}\left(\frac{3\,C_\epsilon}{2\,C_\epsilon-3\,C_s}-l\right),$$

where rhs and lhs refer to the right-hand side and left-hand side of the latter form of the $\overline{v^2}$ equation, and Z stands for $\mathcal{E}|ct-z|/\mathcal{K}^{3/2}$. If the budget is to reduce to the usual balance between time rate of change and diffusion, we must have lhs$\equiv$0 and $n>l-1$. The first condition gives $l=3\,C_\epsilon/(2\,C_\epsilon-3\,C_s)=3m$, which can readily be seen to be contradict the second condition. The other possibility is that rhs$\equiv$lhs, which leads to $n=l-1$ and

$$\frac{1}{3}\left(C_1-1+\frac{C_2\,a_{11}}{3\,C_s}\right)=\left(\frac{C_\epsilon}{2\,C_\epsilon-3\,C_s}\right)^2\frac{\mathcal{V}^2}{\mathcal{K}}\,C_s\,a_{33}.$$

This determines the behavior of $\overline{v^2}$ in the vicinity of the edge through the expressions of l and $\mathcal{V}^2/\mathcal{K}$ given as functions of a_{33} and a_{11}—that remain free. Simple algebra then shows that D_{22} is exactly 2/3 of $\partial\overline{v^2}/\partial t$.

[1] P. G. Saffman, "A model for inhomogeneous turbulent flows," Proc. R. Soc. London, Ser. A **317**, 417 (9170).
[2] H. Vollmers and J. C. Rotta, "Similar solutions of the mean velocity, turbulent energy and length scale equation," AIAA J. **15**, 714 (1977).
[3] A. J. Paullay, R. E. Melnik, A. Rubel, S. Rudman, and M. J. Siclari, "Similarity solutions for plane and radial jets using a k-ϵ turbulence model," Trans. ASME, J. Fluids Eng. **107**, 79 (1985).
[4] F. R. Menter, "Influence of freestream values on k-ω turbulence model predictions," AIAA J. **30**, 1657 (1992).
[5] P. R. Spalart and S. R. Allmaras, "A one-equation turbulence model for aerodynamic flows," AIAA Paper No. 92-0439, 1992.
[6] J.-B. Cazalbou, P. R. Spalart, and P. Bradshaw, "On the behavior of two-equation models at the edge of a turbulent region," Phys. Fluids **6**, 1797 (1994).
[7] S. Corrsin and A. L. Kistler, "Free-stream boundaries of turbulent flows," NACA Report 1244, 1955.
[8] O. M. Phillips, "The irrotational motion outside a free turbulent boundary," Proc. Cambridge Philos. Soc. **51**, 220 (1955).
[9] G. Fabris, "Conditional sampling study of the turbulent wake of a cylinder. Part 1," J. Fluid Mech. **94**, 673 (1978).
[10] E. Gutmark and I. Wygnanski, "The planar turbulent jet," J. Fluid Mech. **73**, 465 (1976).
[11] I. Wygnanski and R. E. Fiedler, "The two-dimensional mixing region," J. Fluid Mech. **41**, 327 (1970).
[12] T. B. Hedley and J. F. Keffer, "Some turbulent/non-turbulent properties of the outer intermittent region of a boundary layer," J. Fluid Mech. **64**, 645 (1974).
[13] J. Murlis, H. M. Tsai, and P. Bradshaw, "The structure of turbulent boundary layers at low Reynolds numbers," J. Fluid Mech. **122**, 132 (1982).
[14] I. P. D. De Silva and H. J. S. Fernando, "Oscillating grids as a source of nearly isotropic turbulence," Phys. Fluids **6**, 2455 (1994).
[15] B. J. Daly and F. H. Harlow, "Transport equations in turbulence," Phys. Fluids **13**, 2634 (1970).
[16] K. Hanjalić and B. E. Launder, "A Reynolds stress model of turbulence and its application to thin shear flows," J. Fluid Mech. **52**, 609 (1972).
[17] G. L. Mellor and H. J. Herring, "A survey of mean turbulent field closure model," AIAA J. **11**, 590 (1973).
[18] J. L. Lumley, "Computational modeling of turbulent flows," Adv. Appl. Mech. **18**, 123 (1978).
[19] J. Rotta, "Statistiche theorie nichthomogener turbulenz *i*," Z. Phys. **129**, 547 (1951).
[20] J.-B. Cazalbou and P. Chassaing, "New results on the model problem of the diffusion of turbulence from a plane source," Phys. Fluids **13**, 464 (2001).
[21] B. Perot and P. Moin, "Shear-free turbulent boundary layers. Part 1 Physical insight into near-wall turbulence," J. Fluid Mech. **295**, 199 (1995).
[22] A. G. Straatman, G. D. Stubley, and G. D. Raithby, "Examination of diffusion modeling using zero-mean-shear turbulence," AIAA J. **36**, 929 (1998).
[23] J. L. Lumley and P. Mansfield, "Second order modeling of turbulent transport in the surface mixed layer," Boundary-Layer Meteorol. **30**, 109 (1984).
[24] M. M. Rogers and R. D. Moser, "Direct simulation of a self-similar turbulent mixing layer," Phys. Fluids **6**, 903 (1994).
[25] T.-H. Shih, J. L. Lumley, and J. Janicka, "Second-order modelling of a variable-density mixing layer," J. Fluid Mech. **180**, 93 (1987).
[26] A. G. Straatman, "A modified model for diffusion in second-moment turbulence closures," Trans. ASME, J. Fluids Eng. **121**, 747 (1999).